

Supporting Information

Table S1: Sampling ranges and window divisions in WTM-eABF calculations. The range of each window is given in Å, with the corresponding simulation time (μ s) listed below.

Membrane	RhoVRs	win01	win02	win03	win04	win05
POPC	RVR1	[10, 55] 4.0	[-15, 15] 5.6	[-55, -10] 4.0	-	-
	SRV1	[10, 55] 4.0	[-15, 15] 4.0	[-55, -10] 2.9	-	-
	RVR1-component	[10, 43] 1.5	[-15, 15] 2.0	[-43, -10] 1.0	-	-
	SRV1-component	[10, 43] 1.5	[-15, 15] 2.0	[-43, -10] 0.5	-	-
	RVR1-protonated	[10, 50] 1.5	[-15, 15] 3.0	[-50, -10] 1.7	-	-
POPC:CHL	RVR1	[13, 43] 3.0	[-15, 15] 5.6	[-43, -13] 1.0	[36, 50] 0.5	[-50, -36] 0.5
	SRV1	[41, 13] 1.5	[-15, 15] 5.4	[-41, -13] 1.0	[36, 50] 0.5	[-50, -36] 0.5
	RVR1-component	[10, 43] 1.0	[-15, 15] 1.0	[-43, -10] 1.0	-	-
	SRV1-component	[10, 43] 1.0	[-15, 15] 2.0	[-43, -10] 1.0	-	-
	RVR1-protonated	[10, 50] 2.0	[-15, 15] 3.8	[-50, -10] 1.8	-	-

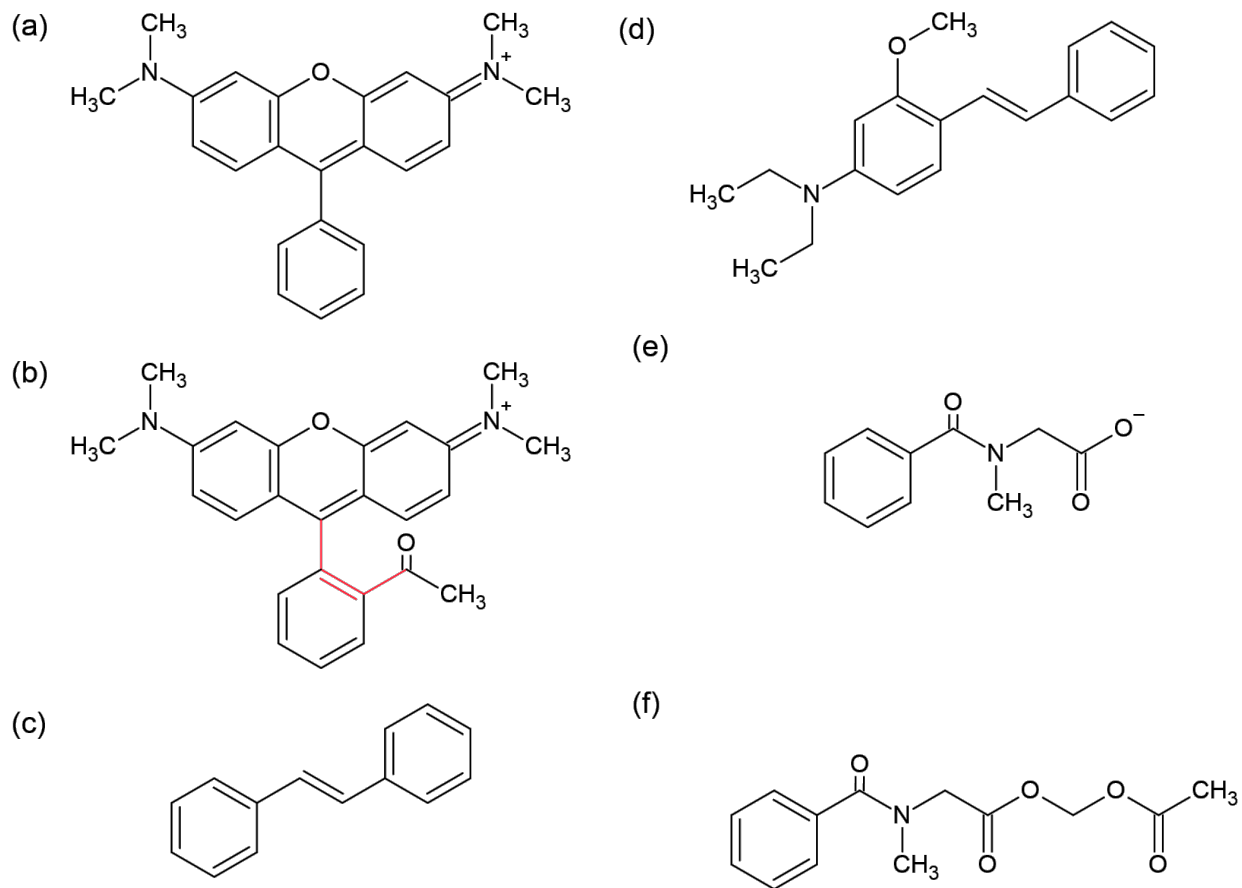


Figure S1: Fragments of RhoVRs employed in their force field parameter optimization (see Methods). Fragment (b) is used to parameterize a dihedral term (highlighted in red) not present in the other components.

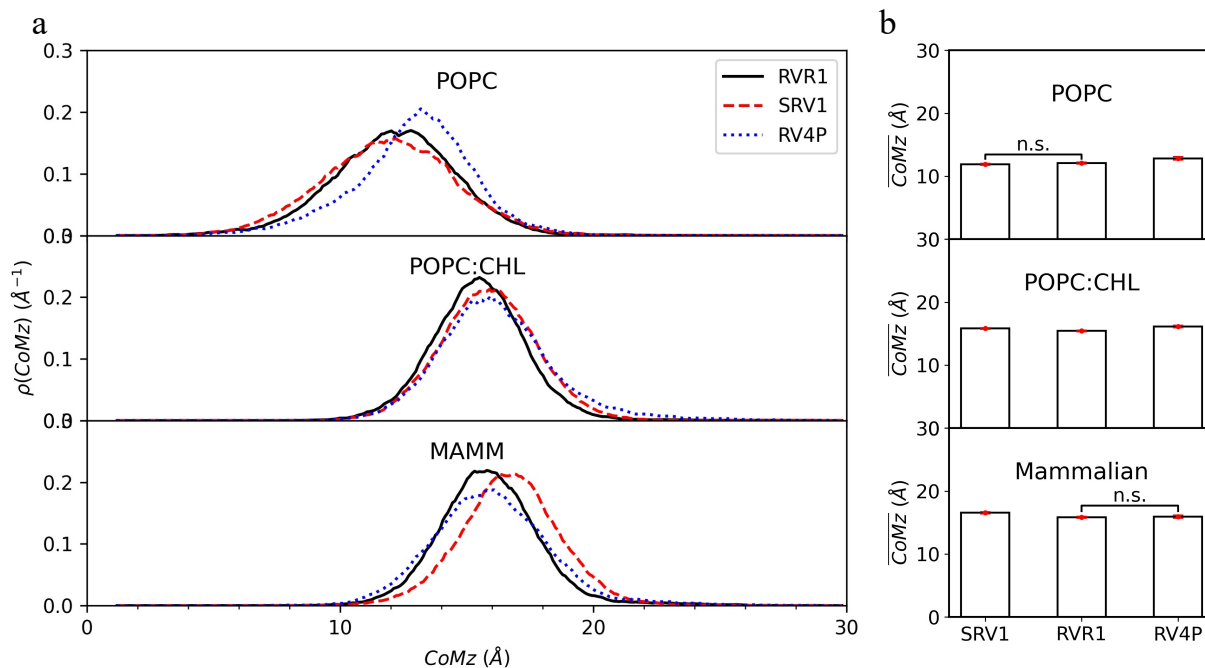


Figure S2: Center of mass of RhoVRs (CoMz) in equilibrium MD simulations. (a) Probability density distribution of CoMz ($\rho(\text{CoMz})$). (b) Average CoMz ($\overline{\text{CoMz}}$) of RhoVR dyes with the standard error of the mean shown as error bars. Statistical significance analyzed by Welch's t -test yields $P < 0.05$ for all pairs of RhoVR dyes in a given lipid environment except for those labeled as *n.s.* (not significant).

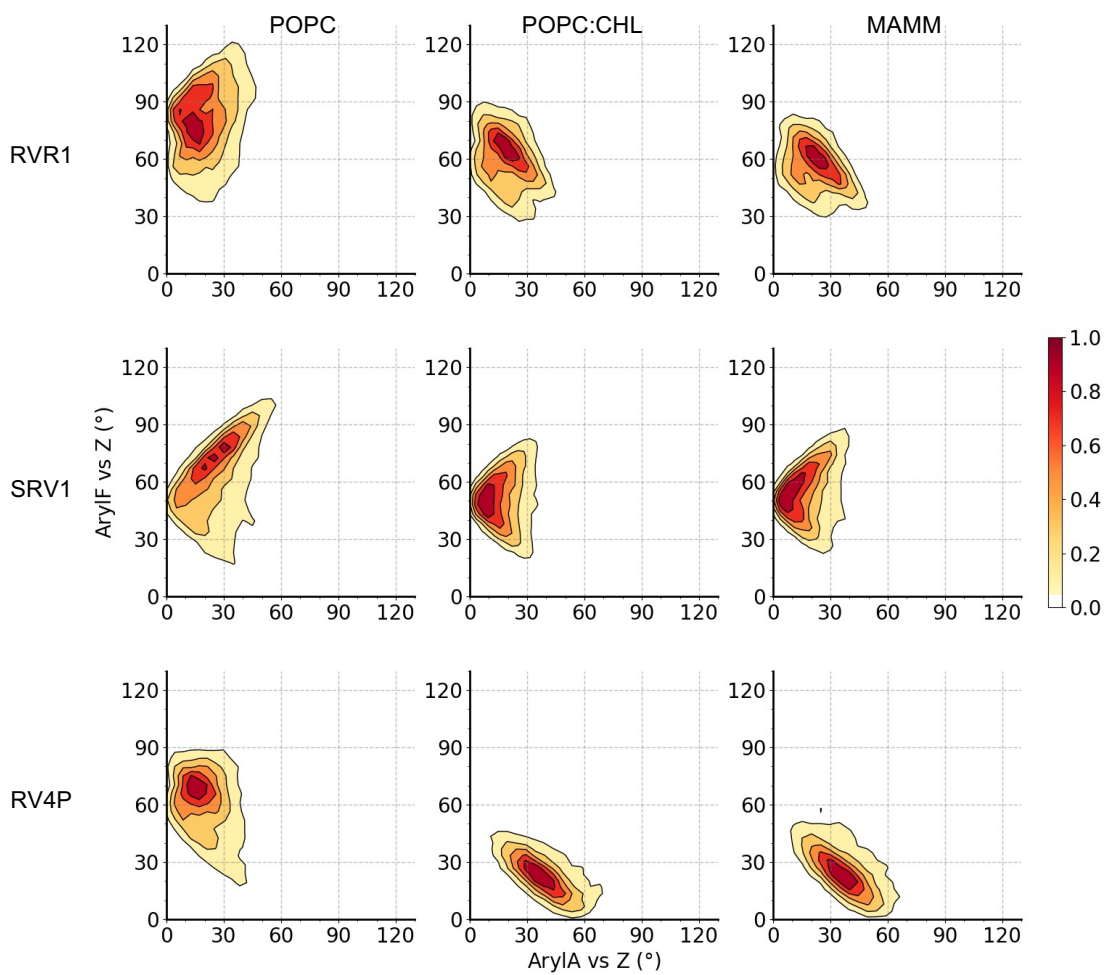


Figure S3: Contour plots depicting the tilt angles of \overrightarrow{ArylA} and \overrightarrow{ArylF} for RhoVR 1, RhoVR 1-4', and SPIRIT RhoVR 1 in equilibrium MD simulations.

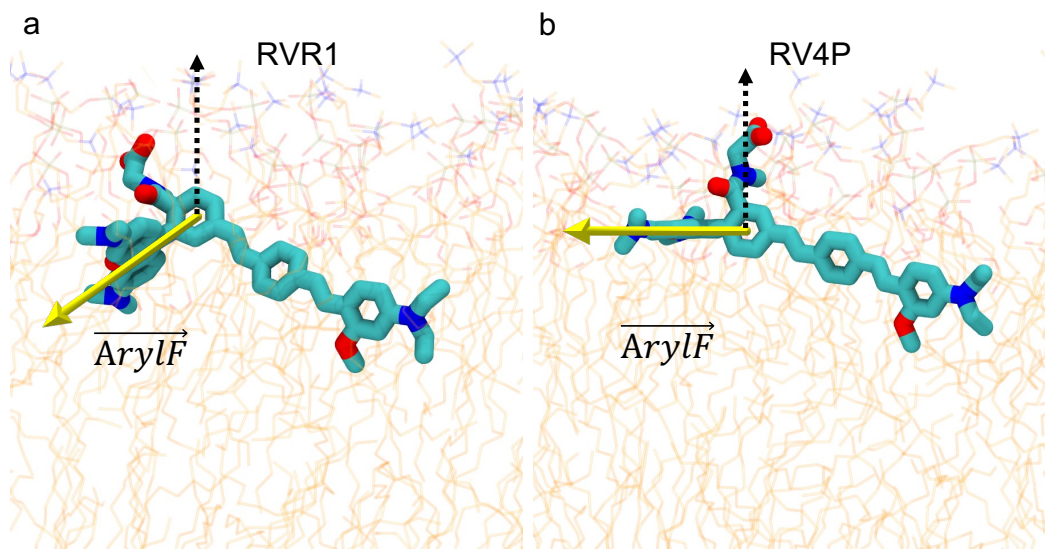


Figure S4: Representative snapshots from equilibrium MD simulations in pure POPC showing the tilting of \vec{ArylF} in RhoVR 1 (a) and RhoVR 1-4' (b). The tilt angles of \vec{ArylF} are $\sim 120^\circ$ and $\sim 90^\circ$ in (a) and (b), respectively.

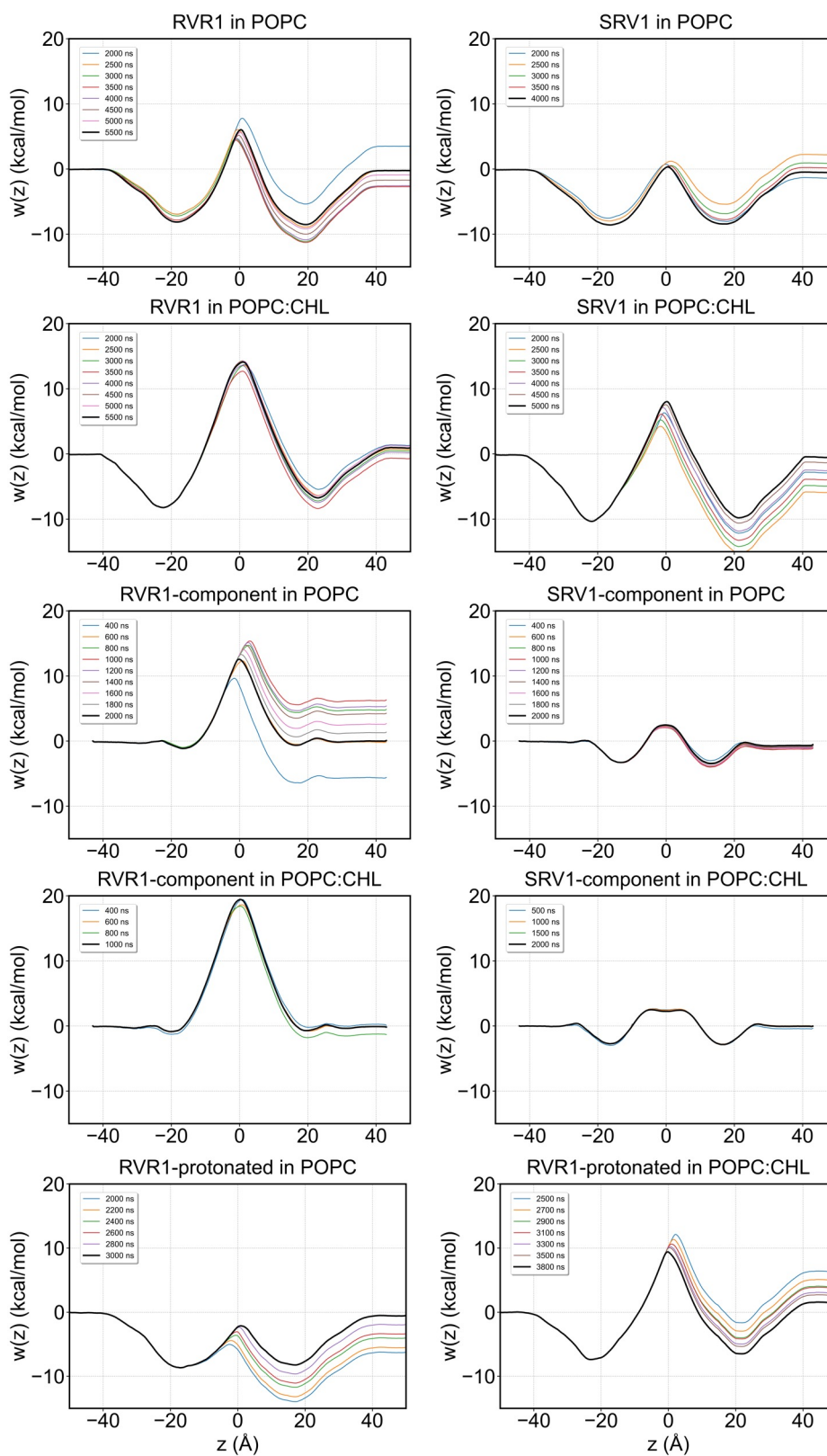


Figure S5: Convergence of unsymmetrized free-energy profiles of RhoVR 1, SPIRIT RhoVR 1 and their components in POPC and POPC:CHL bilayers. Each panel displays PMF profiles calculated at different simulation lengths (per window) with the final profile highlighted in black.

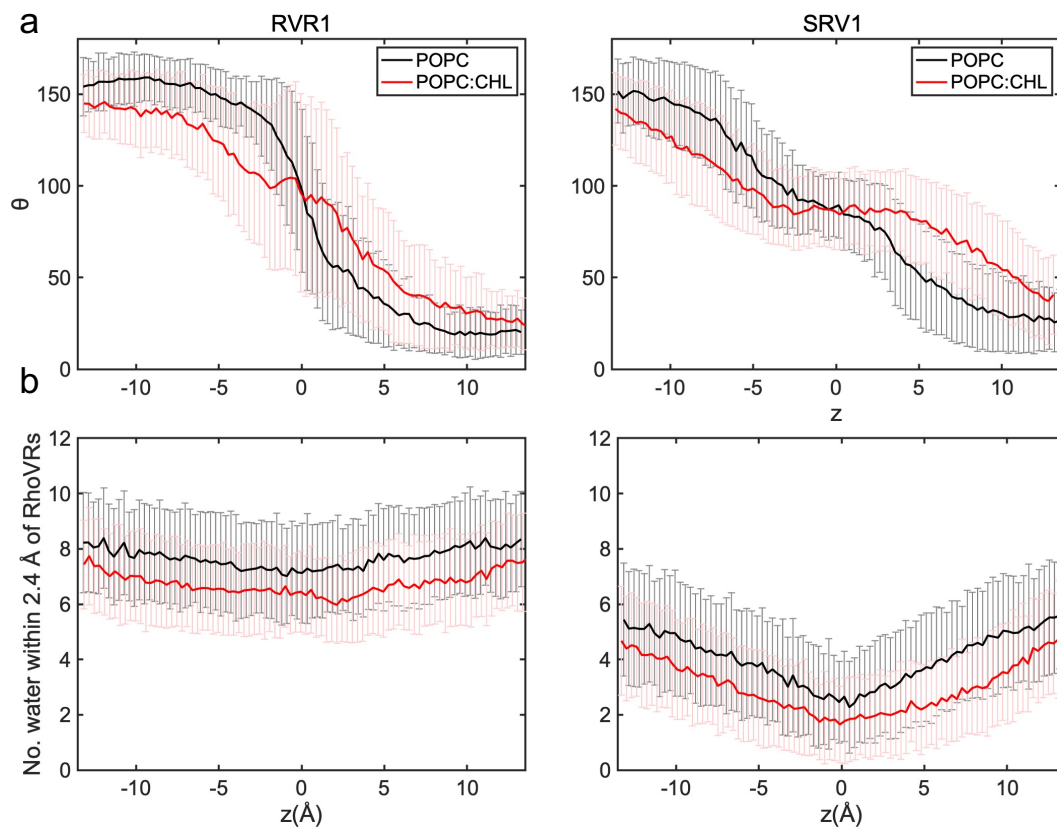


Figure S6: Orientation and solvation of RhoVRs during membrane permeation. (a) RhoVR Orientation as a function of dye location in a given membrane. (b) Average number of water within 2.4 Å of RhoVRs. All panels were computed using the WTM-eABF trajectories with $-15 \text{ \AA} < z < 15 \text{ \AA}$.

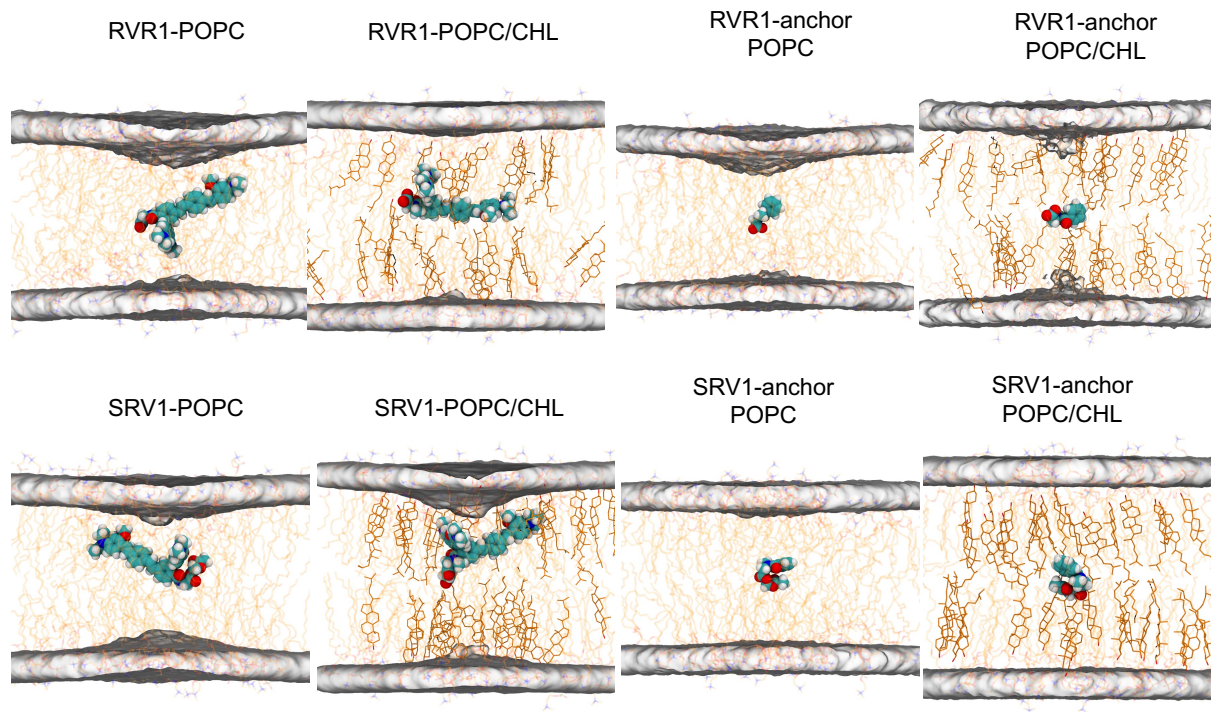


Figure S7: Occupancy of phosphorus atoms calculated from the WTM-eABF trajectories of a given permeant with $-5 \text{ \AA} < z < 5 \text{ \AA}$. The isosurfaces with an isovalue of 3% occupancy are superimposed with representative permeant conformations obtained from root mean square deviation (RMSD)-based clustering analysis.

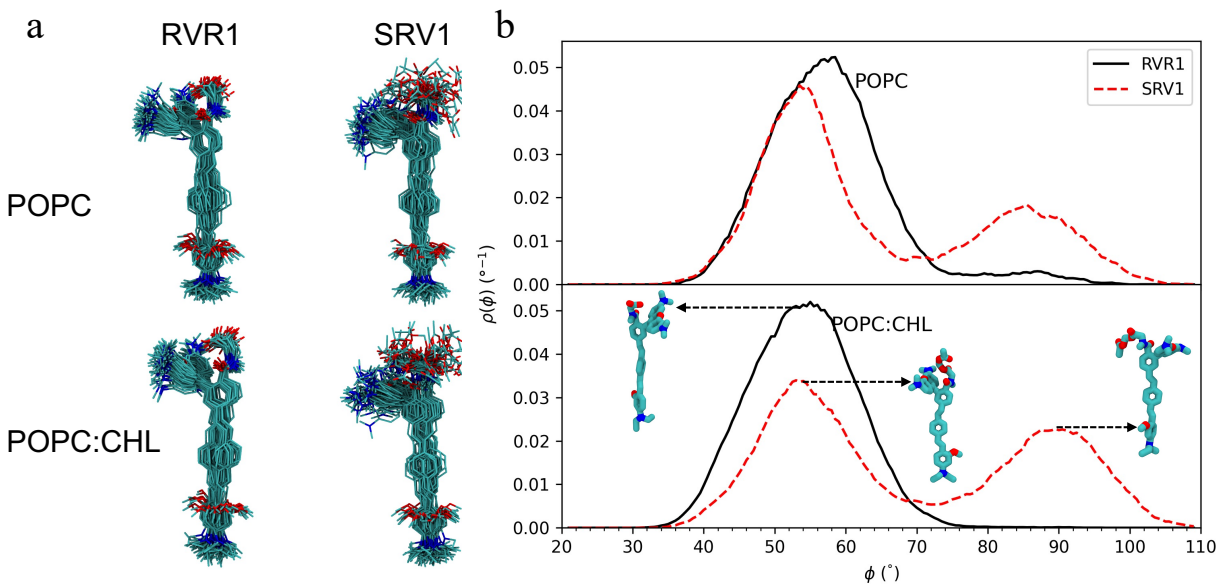


Figure S8: (a) Configurations of RhoVR 1 and SPIRIT RhoVR 1 extracted from WTM-eABF trajectories with $-15 \text{ \AA} < z < 15 \text{ \AA}$. Following alignment by minimizing RMSD, simulation snapshots are taken every 100 ns, resulting in approximately 50 superimposed configurations for each VSD. (b) Probability density distributions of the angle φ between \overrightarrow{ArylF} and \overrightarrow{ArylA} computed from the same trajectories analyzed in (a).